ON THE USE OF BS 7910 OPTION 1 FAD TO NON-METALLIC MATERIALS

Journal:	*Fatigue & Fracture of Engineering Materials & Structures*
Manuscript ID	Draft
Manuscript Type:	Original Contribution
Date Submitted by the Author:	n/a
Complete List of Authors:	Fuentes, Juan Cicero, Sergio; University of Cantabria, Department of Materials Science and Engineering; Ibañez-Gutierrez, Francisco Pessoa, Isabela
Keywords:	Failure criterion, Fracture mechanics, Structural integrity

ON THE USE OF BS 7910 OPTION 1 FAD TO NON-METALLIC MATERIALS

J. D. Fuentes, S. Cicero*, F. T. Ibáñez-Gutiérrez, I. Procopio

LADICIM (Laboratory of Materials Science and Engineering), University of Cantabria, E.T.S. de Ingenieros de Caminos, Canales y Puertos, Av/ Los Castros 44, 39005, Santander, Cantabria, Spain

*corresponding author: ciceros@unican.es

ABSTRACT

This paper provides a structural integrity assessment methodology for the analysis of non-metallic materials. The approach uses the BS 7910 Option 1 Failure Assessment Diagram, originally proposed for the fracture-plastic collapse assessment of metallic materials. The methodology has been applied to 60 fracture specimens, combining twelve different materials and covering polymers, composites and rocks. The results obtained validate the proposed assessment methodology and demonstrate its safety for the materials analysed here.

Keywords

Failure criterion; Fracture Mechanics; Structural Integrity

Nomenclature

a	crack length
A_p	plastic area under the load-displacement curve in a fracture test
b_0	initial remaining ligament
B	specimen thickness
e_{max}	strain under maximum load
E	elastic modulus
$f(L_r)$	function of L_r defining FAD
J	J integral
J_e	elastic component of J
K_{mat}	material fracture resistance measured by stress intensity factor
K_I	stress intensity factor
K_{IC}	fracture toughness
K_r	fracture ratio of applied K_I to fracture resistance
L_r	ratio of applied load to limit load
P	applied load
P_L	limit load
N	strain hardening exponent
η	dimensionless constant
W	specimen width
σ_u	ultimate tensile strength
$\sigma_{0.2}$	0.2% proof strength
FAD	Failure Assessment Diagram
FAL	Failure Assessment Line
PMMA	Polymethylmethacrylathe
SGFR-PA6	Short glass fibre reinforced polyamide 6

1. INTRODUCTION

A considerable number of structural failures are associated to the presence of crack-like defects. In order to avoid or predict such failures, structural integrity assessment procedures[1-4] make wide use of fracture mechanics concepts and derivative tools such as Failure Assessment Diagrams (FADs).

Until now, most structural integrity assessment procedures have only addressed the prediction of the fracture-plastic collapse of metallic materials. For example, FITNET FFS Procedure[1] states the following in the introduction of the Fracture Module (Section 6): "*The FITNET Fracture Module described in this section is based on fracture mechanics principles and is applicable to the assessment of metallic structures (with or without welds) containing actual or postulated flaws. The purpose of the analysis in this Module is to determine the significance, in terms of fracture and plastic collapse, of flaws postulated or present in metallic structures and components*". Similarly, the Scope section of BS7910[2] states that "*This British Standard gives guidance and recommendations for assessing the acceptability of flaws in all types of structures and components. Although emphasis is placed on welded fabrications in ferritic and austenitic steels and aluminium alloys, the procedures may be used for analysing flaws in structures made from other metallic materials and in non-welded components or structures*". However, the increasing use of new non-metallic materials on structural applications makes it necessary to develop structural integrity assessment tools for these types of materials.

Thus, the main objective of this paper is to evaluate the use of the BS 7910 Option 1 FAD[2] for non-metallic materials. With this purpose, section 2 provides an overview of the FADs and the different FAD options within the BS 7910, section 3 describes the experimental programme (materials and methods), section 4 shows the results obtained and, finally, section 5, presents the corresponding conclusions.

2. FAILURE ASSESSMENT DIAGRAMS AND BS7910 ANALYSIS OPTIONS

2.1 FAILURE ASSESSMENT DIAGRAMS

Failure Assessment Diagrams (FADs) are one of the main engineering tools for the assessment of fracture-plastic collapse in cracked components[1-4]. These diagrams allow the simultaneous assessments of

fracture and plastic collapse to be made by using two normalised parameters, K_r and L_r, whose expressions are:

$$K_r = \frac{K_I}{K_{mat}} \quad (1)$$

$$L_r = \frac{P}{P_L} \quad (2)$$

K_r evaluates the component against fracture and it is defined by the ratio of K_I to K_{mat}, K_I being the stress intensity factor, and K_{mat} being the material fracture resistance measured by the stress intensity factor (e.g.; K_{IC}, K_{JC}, K_{JIC}, etc.)[5,6]. L_r evaluates the component against plastic collapse and it is defined by the ratio P to P_L, P being the applied load and P_L being the limit load.

Once the assessment point representing the cracked component being analysed is described by the K_r and L_r coordinates, it is necessary to define the limiting conditions. This is done by defining the Failure Assessment Line (FAL). Finally, if the assessment point is located above the FAL, the component is considered to be under unsafe conditions, whereas if the assessment point is located below the FAL, this means that the component is considered to be under safe conditions. The critical situation (failure condition) is that in which the assessment point lies exactly on the FAL. Fig. 1[1] shows an example with the three different possible situations.

2.2 BS 7910 ANALYSIS OPTIONS

The general expression for the FAL in BS 7910 and other procedures is:

$$K_r = f(L_r) \quad (3)$$

The $f(L_r)$ functions are actually plasticity corrections to the fracture assessment ($K_I = K_{mat}$), whose exact analytical solution is:

$$f(L_r) = \sqrt{\frac{J_e}{J}} \quad (4)$$

J being the applied J-integral and J_e being its corresponding elastic component. This FAL corresponds to BS 7910 Option 3 FAD [2] and FITNET FFS Procedure Option 4 [1,7]. In practice, structural integrity assessment procedures[1-4] provide approximate solutions to (4), which are defined through the tensile properties of the material. These approximate solutions are generally provided hierarchically, that is, defining different levels on which the more defined the material stress-strain curve, the more approximate are such solutions to (4). For example, BS 7910 [2] defines Option 1, which requires both the yield or proof strength and the ultimate tensile strength. For materials exhibiting continuous yielding behaviour, Option 1 is defined by equations (5) to (10) (this FAD coincides with FITNET FFS Procedure Option 1 [1]):

$$K_r = f(L_r) = \left[1 + \frac{1}{2}(L_r)^2\right]^{-1/2} \cdot \left[0.3 + 0.7 \cdot e^{-\mu\cdot(L_r)^6}\right] \qquad L_r \leq 1 \tag{5}$$

$$K_r = f(L_r) = f(1) \cdot L_r^{\frac{N-1}{2N}} \qquad 1 < L_r \leq L_{r,max} \tag{6}$$

$$K_r = f(L_r) = 0 \qquad L_r = L_{r,max} \tag{7}$$

$$\mu = min\left[0.001 \cdot \frac{E}{\sigma_y}; 0.6\right] \tag{8}$$

$$N = 0.3 \cdot \left(1 - \frac{\sigma_y}{\sigma_u}\right) \tag{9}$$

$$L_{r,max} = \frac{\sigma_y + \sigma_u}{2 \cdot \sigma_y} \tag{10}$$

The μ and N parameters follow expressions (equations (8) and (9), respectively) that have been calibrated and validated for metallic materials [8-11], but not for non-metallic ones. This is the main reason why

structural integrity procedures such as FITNET FFS Procedure and BS7910 do not cover the fracture assessment of non-metallic materials.

On the other hand, BS 7910 Option 2 or FITNET FFS Procedure Option 3 requires the full stress-strain curve and is defined by equations (11) to (13):

$$f(L_r) = \left(\frac{E\varepsilon_{ref}}{L_r\sigma_y} + \frac{L_r^3\sigma_y}{2E\varepsilon_{ref}}\right)^{-1/2} \qquad L_r < L_{r,max} \qquad (11)$$

where ε_{ref} is the true strain at the true stress $\sigma_{ref} = L_r\sigma_y$

$$f(L_r) = 0 \qquad L_r > L_{r,max} \qquad (12)$$

L_{rmax} also follows equation (10)

Option 1 FAD is, therefore, the most simple analysis option of BS 7910 and, in practice, it is the most widely used by industry. However the main structural integrity assessment procedures[1-4], and particularly, the BS 7910, specifically state that their application is limited to metallic materials. Thus, the structural integrity assessment of non-metallic components cannot, in principle, be performed by using such codes or documents.

3. MATERIALS AND METHODS

The possibility of using FADs for the structural integrity assessment of non-metallic components has been analysed in the following materials and specimens:

- PMMA: 3 Single Edge Notched Bending (SENB) specimens (see Fig. 2) [12-14]. As shown by Cicero et al. [13], PMMA cracked specimens developed a basically linear-elastic behaviour until final failure. The fracture surface had a brittle aspect, with a clear distinction of the mirror zone or mirror region, which is a zone where thin planar crazes form a flat smooth fracture origin associated to slow crack growth. Because of the presence of a thin layer of highly oriented polymer (crazing) with a different

refractive index from that of the bulk, interference colour fringes, identified in Cicero et al.[13] as ‘‘initiation lines’’, were observed in the mirror region. The resulting broken surface is quite smooth (see Cicero et al.[13] for further details). Table 1 shows the mechanical properties of the material, obtained as the average values from two tensile tests performed following ASTM D638 [15].

- Granite: 6 Single Edge Notched Bending (SENB) specimens (see Fig. 3) [16]. The behaviour of the specimens was again brittle. In all tests, fracture took place across the middle plane of the specimens, starting from the crack tip. The fracture surfaces were basically flat and had a brittle aspect (see Cicero et al.[16]] for further details). The main mechanical properties of the material are shown in Table 1, obtained as the average values from six splitting tensile tests (Brazilian test) performed following UNE 22590 [17, 18]. The splitting tensile test provides an indirect measurement of the tensile strength of rocks. It generates tensile failure of cylindrical rock specimens by subjecting such specimens to compressive force along two opposite generatrixes. Specimens usually have a 54 mm diameter and a height-to-diameter ratio of 2.5 to 3.0. The sample is positioned horizontally and loaded in compression until its flat ends split, with the material corresponding tensile strength being directly related with the failure load and the specimen geometry. Details may be found in the corresponding standards [17,18].

- Oolitic limestone: 6 Single Edge Notched Bending (SENB) specimens (see Fig. 3) (see Cicero et al. [16]). Fracture characteristics were similar to those mentioned above for the granite specimens. The main mechanical properties of the material are shown in Table 1, obtained as the average values from six splitting tensile tests (Brazilian test) performed following UNE 22590 [17,18].

- Polyamide 6: 5 Single Edge Notched Bending (SENB) specimens (tested in 3-points) (see Fig. 2 and Ibañez-Gutiérrez et al. [19]. Mechanical properties were obtained as the average values from two tensile tests performed following ASTM D638 [15], and are shown in Table 1. All the specimens (tensile and fracture) were tested in dry conditions (0% moisture).

- Short glass fibre reinforced polyamide 6 (SGFR-PA6) (5 wt. %): 5 Single Edge Notched Bending (SENB) specimens (tested in 3-points) (see Fig. 2) [19]. The fracture resistance of the specimens presented significant scatter [19]. Those specimens with the lowest fracture resistance had a brittle aspect, and presented the typical fracture pattern for cracked polymers, with the following zones: mirror zone (smooth and flat surface around the initiation point), mist zone (flat smooth area

surrounding the mirror region that shows a slight change in the surface texture) and deformation zone (whose texture is directly related to the type of loading and the applied stress). On the other hand, those specimens with higher fracture resistance presented multiple imitation areas, a rougher texture and presence of dimples, which are an indication of non-linear (tougher) micromechanisms [19]. The mechanical properties were obtained as the average values from two tensile tests performed following ASTM D638 [15], and are shown in Table 1. All the specimens (tensile and fracture) were tested in dry conditions

- Short glass fibre reinforced polyamide 6 (10 wt. %): 5 Single Edge Notched Bending (SENB) specimens (tested in 3-points) (see Fig. 2) [19]. The evolution in the fracture micromechanisms is evident when the fibre content increases (from 0 wt. % up to 50 wt% fibre content) [19]: while there is a basically global brittle aspect in polyamide 6 specimens, there is an increasing rougher and more non-linear aspect when the fibre content increases. This evolution in the fracture micromechanisms is in agreement with the corresponding reported increase in the fracture resistance [19]. The mechanical properties were obtained as the average from two tensile tests performed following ASTM D638 [15], and are also shown in Table 1. All the specimens (tensile and fracture) were tested in dry conditions
- Short glass fibre reinforced polyamide 6 (30 wt. %): 5 Single Edge Notched Bending (SENB) specimens (tested in 3-points) (see Fig. 2) [19]. The mechanical properties were obtained as the average values from two tensile tests performed following ASTM D638 [15] (see Table 1). All the specimens (tensile and fracture) were tested in dry conditions
- Short glass fibre reinforced polyamide 6 (50 wt. %): 5 Single Edge Notched Bending (SENB) specimens (tested in 3-points) (see Fig. 2) [19]. Table 1 shows the corresponding mechanical properties, obtained as the average values from two tensile tests performed following ASTM D638 [15]. All the specimens (tensile and fracture) were tested in dry conditions.
- Short glass fibre reinforced polyamide 6 (10 wt. %) and 2% moisture content: 5 Single Edge Notched Bending (SENB) specimens (tested in 3-points) (see Fig. 2). Table 1 shows the corresponding mechanical properties, obtained as the average values from two tensile tests performed following ASTM D638 [15]. In this case (and also in the following ones where the specimens contain different amounts of moisture), it is observed that the introduction of moisture in SGFR-PA6 reduces the material strength and increases its ductility. These specimens, and the ones gathered below with

different combinations of moisture and fibre contents, have been specifically tested for the analysis performed in this paper.

- Short glass fibre reinforced polyamide 6 (10 wt. %) and 5% moisture content: 5 Single Edge Notched Bending (SENB) specimens (tested in 3-points) (see Fig. 2). Table 1gathers the corresponding mechanical properties, also obtained as the average values from two tensile tests performed following ASTM D638 [15].
- Short glass fibre reinforced polyamide 6 (50 wt. %) and 2% moisture content: 5 Single Edge Notched Bending (SENB) specimens (tested in 3-points) (see Fig. 2). The corresponding mechanical properties are shown in Table 1, and were obtained as the average values from two tensile tests performed following ASTM D638 [15].
- Short glass fibre reinforced polyamide 6 (50 wt. %) and 4% moisture content: 5 Single Edge Notched Bending (SENB) specimens (tested in 3-points) (see Fig. 2). Table 1 shows the corresponding mechanical properties, obtained as the average values from two tensile tests performed following ASTM D638 [15].

The corresponding stress-strain curves are shown in Fig. 4.

Table 2 shows the fracture loads of the different specimens.

Concerning the material fracture toughness, the above mentioned specimens were tested following [20], in the case of polymers and dry composites, and [21] in the case of rocks. For the case of SGFR-PA6 materials with moisture contents, the observed fracture behaviour had a significant plastic component, so the fracture resistance was measured following [6,22].

The K_I expression for Single Edge Notched Bending (tested in 3-points) (PMMA, PA6 and dry SGFR-PA6 (5, 10, 30, 50 wt. %)) is [20]:

$$K_I = \frac{P}{B\sqrt{W}} \frac{3\frac{S}{W}\sqrt{\frac{a}{W}}}{2\left(1+\frac{2a}{W}\right)\left(1-\frac{a}{W}\right)^{3/2}} \left[1{,}99 - \frac{a}{W}\left(1-\frac{a}{W}\right)\left(2{,}15 - 3{,}93\left(\frac{a}{W}\right) + 2{,}70\left(\frac{a}{W}\right)^2\right)\right] \quad (13)$$

where P is the applied load, B is the specimen thickness, a is the crack length and W is the specimen width.

For SGFR-PA6 (10, 50 wt. %) with different moisture contents (2%, 4% or 5%), K_{mat} was obtained from:

$$K_{mat} = \sqrt{J_{mat}\frac{E}{1-\upsilon^2}} \tag{14}$$

J_{mat} is the J-integral at onset of fracture, E is the Young´s modulus and υ is the Poisson´s ratio [22], J_{mat} is obtained from equation (15):

$$J_{mat} = J_e + J_p = \frac{(1-\upsilon^2)(K_I)^2}{E} + \frac{\eta A_p}{B b_0} \tag{15}$$

J_e and J_p are, respectively, the elastic and plastic components of J_{mat}, η is a dimensionless constant [22], A_p is the plastic area under the corresponding load-displacement curve (e.g., Fig. 5), b_0 is the initial remaining ligament, B the specimen thickness and K_I is elastic stress intensity factor at instability (equation (13)).

There are several methodologies for the assessment of fracture toughness in rocks [21-28]. The methodology that has been selected here to determine this material property was originally proposed by Srawley and Gross [21]. The expression for Single Edge Notched Bending (tested in 4-points) (granite and oolitic limestone) is:

$$K_I = \frac{F * Y}{b * h^{1/2}} \tag{16}$$

where:

$$Y = \frac{3 * (L_0 - L_i) * \alpha_0^{1/2} * X}{2h * (1 - \alpha_0)^{3/2}} \quad (17)$$

$$X = 1{,}9887 - \left[\frac{(3{,}49 - 0{,}68\alpha_0 - 1{,}35\alpha_0^2) * \alpha_0 * (1 - \alpha_0)}{(1 + \alpha_0)^2}\right] - 1{,}32\alpha_0 \quad (18)$$

F is the applied load, b is the remaining ligament, h is the height of the specimen, L_0 and L_i are the spans between the outer and inner loading points, respectively, a is the crack length and $\alpha_0 = a_0/h$. Here, it should be noted that size effects [30-32], which are a key issue in rock fracture mechanics, are not directly addressed in this work, so that the obtained material parameters and analytical results (together with the subsequent conclusions) may not be transferable to different scales (e.g., massive rocks).

Fig. 6 shows the values of fracture resistance of the different non-metallic materials being analysed. It can be observed how this parameter tends to increase with moisture content in SGFR-PA6 (10 wt. %), whereas it clearly decreases with moisture content in SGFR-PA6 (50 wt. %).

4. DEFINITION OF BS 7910 OPTION 1 FAD FOR NON METALLIC MATERIALS

In the same way as it was done for metals, the parameters μ and N, used in BS 7910 Option 1 FAD [2], should be defined for non-metallic materials.

In order to characterize μ, equation (8) guarantees that the results obtained by BS 7910 Option 1 [2] FAD are more conservative than those obtained by the more accurate analytical solution provided by BS 7910 Option 2 FAD [2]. The exact μ values can be obtained by using the following expressions [8,9], which are derived by obliging equation (5) (FAD Option 1) to be lower or equal to equation (11) (FAD Option 2):

$$\left[\frac{3}{2}\right]^{-1/2} \cdot [0.3 + 0.7 \cdot e^{-\mu}] \leq \left[ß + \frac{1}{2ß}\right]^{-1/2} \quad (19)$$

where:

$$ß = 1 + \frac{E}{\sigma_y} 0.002 \quad (20)$$

Fig. 7 shows the safe estimate associated to BS7910 FAD Option 1 (equation (8)) and the corresponding points of the non-metallic materials being analysed. The points are located below the curve provided by equation (8), so this equation (used by BS7910 as a safe estimate for metallic materials) is also a safe estimate for the non-metallic materials analysed here. This figure also shows the original points used for the fitting, all of them associated to metallic materials [8,9].

Similarly, equation (9) defines a lower envelope of the strain hardening exponent (N) of a number of steels [9]. The experimental results of the strain hardening exponent (N) for the non-metallic materials analysed here have been obtained by using the Hollomon equation, the results being shown in Table 3. In Fig. 8, it can be seen that the experimental results of the strain hardening exponent (N) obtained by using the Hollomon equation are more conservative than those values proposed by [10, 11]. It can be observed that the 0.3 factor from Equation (9) could be slightly increased in the materials being studied. Assuming a factor of 0.3 is, therefore, a conservative practice.

With all this, it can be concluded that both equations (8) and (9) provide conservative estimations of μ and N, respectively, in the non-metallic materials analysed here. Thus, the use of BS 7910 Option 1 FAD is safe for such materials.

5. VALIDATION: BS 7910 OPTION 1 ANALYSIS OF NON-METALLIC MATERIALS

In section 2, K_r was defined as the ratio of K_I to K_{mat}, and L_r was defined as the ratio of P to P_L.

The values of K_I for Single Edge Notched Bending (tested in 3-points) can be obtained by the application of equation (13), while the K_I values for Single Edge Notched Bending (tested in 4-points) may be obtained by using equations (16) to (18).

On the other hand, the values of K_{mat} usually considered in structural integrity assessments correspond to a 95% confidence level (or similar). This, assuming a normal distribution, is equal to the mean (the average of the experimental values of the fracture resistance for each particular material, $K_{mat,avg}$) minus 1645 times the standard deviation of the K_{mat} tests results obtained on each material (equation (21)):

$$K_{mat95\%} = K_{mat,avg} - 1.645 \cdot stv\,(K_{mat}) \quad (21)$$

The applied load (P) is shown in Table 2, and it corresponds to the fracture load obtained by testing the specimens.

In order to determinate the limit load (P_L), it is necessary to distinguish between plane strain and plane stress situations.

Plane strain conditions dominate when equation (22) is fulfilled [33]:

$$K_{mat} < \sigma_Y \cdot \left(\frac{B}{2.5}\right)^{1/2} \tag{22}$$

In this case, the limit load may be defined by equation (23):

$$P_L = \frac{1.408 \cdot \left(1-\frac{a}{W}\right)^2 \cdot W^2 \cdot B \cdot \sigma_y}{S} \tag{23}$$

Where a is the crack size, W is the specimen width, b is the remaining ligament, B is the thickness of the specimen, σ_y is the yield stress or proof stress, and S is the span of the specimen.

On the other hand, plane stress conditions dominate when equation (24) is fulfilled [34]:

$$K_{mat} > \sigma_Y \cdot (\pi B)^{1/2} \tag{24}$$

The corresponding limit load is given by:

$$P_L = \frac{1.072 \cdot \left(1-\frac{a}{W}\right)^2 \cdot W^2 \cdot B \cdot \sigma_y}{S} \tag{25}$$

These two solutions of P_L (plane strain and plane stress) are where taken from R6 Procedure [3], given that BS7910 [2] does not explicitly provide solutions of P_L for SENB specimens.

If the K_{mat} value is located between plane strain conditions and plane stress conditions, the value of P_L should be defined by interpolating both values (plane strain - plane stress values).

Fig. 9 presents the results obtained for the structural integrity assessment of the twelve non-metallic materials studied here when applying the FAD methodology. All the assessment points at failure correspond to safe structural integrity evaluations, given that there are no assessment points within the safe area.

6. CONCLUSIONS

This paper suggests the applicability of BS 7910 Option 1 FAD for the structural integrity assessment of non-metallic materials, validating its use for twelve different materials. The experimental programme is composed of 60 fracture specimens, combining 12 different non-metallic materials (PMMA, granite, oolitic limestone, PA6 and SGFR-PA6 (5, 10, 30, 50 wt. %)) in dry conditions and SGFR-PA6 (10, 50 wt. %) with different moisture contents.

The values of the FAD fitting parameters (μ and N) used in BS 7910 Option 1, originally defined for metallic materials, may also be used for the non-metallic materials analysed here, providing a safe estimate of their actual values.

The application of BS 7910 Option 1 FAD to the non-metallic materials analysed here (covering polymers, composites and rocks) has provided safe assessments.

ACKNOWLEDGEMENTS

The authors of this work would like to express their gratitude to the Spanish Ministry of Economy, Industry and Competitiveness for the financial support of the Project MAT2014-58443-P: “Análisis del comportamiento en fractura de componentes estructurales con defectos en condiciones debajo confinamiento tensional”, on the results of which this paper is based.

REFERENCES

[1] Kocak M, Webster S, Janosch JJ, Ainsworth RA, Koers R (2008). *FITNET fitness-for-service (FFS), Procedure Vol. 1*. GKSS, Hamburg, Germany.

[2] *BS 7910:2013- Guide to methods for assessing the acceptability of flaws in metallic structures* (2013). British Standard Institution, London, UK.

[3] *R6. Assessment of the integrity of structures containing defects. Rev 4* (2007). British Energy Generation Limited, Gloucester, UK.

[4] *API 579-1/ASME FFS-1, Fitness-for service* (2007). American Society of Mechanical Engineers, New York, USA.

[5] *ASTM E399-12e3, Standard Test Method for Linear-Elastic Plane-Strain Fracture Toughness KIc of Metallic Materials* (2012). American Society for Testing and Materials, Philadelphia, USA.

[6] *ASTM E1820-15ae1, Standard Test Method for Measurement of Fracture Toughness* (2015). American Society for Testing and Materials, Philadelphia, USA.

[7] Gutiérrez-Solana F, Cicero S (2009). FITNET FFS procedure: A unified European procedure for structural integrity assessment. *Eng. Fail. Anal.,* 16, 557-577.

[8] Ruiz Ocejo J, Gutiérrez-Solana F, González-Pereda MA (1998). *Report/SINTAP/UC/06: Structural integrity assessment procedures for European industry (SINTAP)*. Santander, Spain.

[9] Ainsworth RA, Gutiérrez-Solana F, Ruiz Ocejo J. (2000). Analysis levels with the SINTAP defect assessment procedures. *Eng. Fract. Anal.*, 67, 515-527.

[10] Ruiz Ocejo J, Gutiérrez-Solana F, González-Pereda MA (1998). *Report/SINTAP/UC/08: Structural integrity assessment procedures for European industry (SINTAP)*. Santander, Spain.

[11] Bannister AC, Ruiz Ocejo J, Gutiérrez-Solana F (2000). Implications of the yield stress/tensile stress ratio to the SINTAP failure assessment diagrams for homogeneous materials. *Eng. Fract. Anal.,* 67, 547-562.

[12] Cicero S, Madrazo V, García T (2015). On the assessment of U-shaped notches using Failure Assessment Diagrams and the Line Method: Experimental overview and validation. *Theor. Appl. Fract. Mech.*, 80, 235-241.

[13] Cicero S, Madrazo V, Carrascal IA (2012). Analysis of notch effect in PMMA by using the Theory of Critical Distances. *Eng. Fract. Mech.*, 86, 56–72.

[14] Cicero S, Madrazo V, Carrascal IA, Cicero R (2011). Assessment of notched structural components using Failure Assessment Diagrams and the Theory of Critical Distances. *Eng. Fract. Mech.,* 78, 2809-2825.

[15] *ASTM D638-10, Standard Test Method for Tensile Properties of Plastics* (2004). American Society for Testing and Materials, Philadelphia, USA.

[16] Cicero S, García T, Castro J, Madrazo V, Andres D (2014). Analysis of notch effect on the fracture behaviour of granite and limestone: an approach from the Theory of Critical Distances. *Eng. Geol.,* 177, 1–9.

[17] *UNE 22950-2:1990, Propiedades mecánicas de las rocas. Ensayos para la determinación de la resistencia Parte 2: resistencia a tracción, Determinación indirecta (ensayo brasileño)* (1990). AENOR, Madrid, Spain.

[18] *UNE-EN 1926:2007, Métodos de ensayo para la piedra natural. Determinación de la resistencia a la compresión uniaxial* (2007). AENOR, Madrid, Spain.

[19] Ibáñez-Gutiérrez FT, Cicero S, Carrascal IA, Procopio I (2016). Effect of fibre content and notch radius in the fracture behaviour of short glass fibre reinforced Polyamide 6: an approach from the Theory of Critical Distances. *Compos. Part B Eng.,* 94, 299-311.

[20] ASTM D5045-99 (2007) e1, Standard Test Methods for Plane-Strain Fracture Toughness and Strain Energy Release Rate of Plastic Materials (2007). American Society for Testing and Materials, Philadelphia, USA.

[21] Srawley J, Gross B (1976). Cracks and fracture. *ASTM Spec. Tech. Publ.,* 601, 559-579.

[22] Wong SC, Mai YW (1999). Essential fracture work of short fiber reinforced polymer blends. *Polymer Eng. Sci.,* 39, 356-364.

[23] Amaral PM, Guerra Rosa L, Cruz Fernandes J (2008). Assessment of fracture toughness in ornamental stones. *Int. J. Rock Mech. Min. Sci.,* 45, 554-563.

[24] *CEN/TS 14425-1:2003, Advanced technical ceramics-test methods for determination of fracture toughness of monolithic ceramics-part1: guide to test method selection* (2003). European Committee for Standardization, Brussels, Belgium.

[25] *ASTM-PS70:1997, Provisional test methods for determination of fracture toughness of advanced ceramics at ambient temperatures* (1997). American Society for Testing and Materials, Philadelphia, USA.

[26] Fowll RJ, Xu C (1993). The cracked chevron-notched Brazilian disc test-geometrical considerations for practical rock fracture-toughness measurement. *Int. J. Rock Mech. Min. Sci. Geomech. Abastr.,* 30, 821-824.

[27] Hashida T, Takahashi H (1993). Significance of AE crack monitoring in fracture-toughness evaluation and nonlinear rock fracture-mechanics. *Int. J. Rock Mech. Min. Sci. Geomech. Abastr.*, 30, 47-60.

[28] Lim IL, Johnston IW, Choy SK, (1994).Assessment of mixed-node fracture toughness testing methods for rocks. *Int. J. Rock Mech. Min. Sci. Geomech. Abastr.,* 79, 363-379.

[29] Ouchterlony F (1988). ISRM suggested methods for determining the fracture-toughness of rock. *Int. J. Rock Mech. Min. Sci. Geomech. Abastr.*, 25, 71-96.

[30] Bazant ZP (1984). Size effect in blunt fracture: concrete, rock, metal. *J. Eng. Mech.* 110 (1984) 518–535.

[31] Bazant ZP (1997). Scaling of quasibrittle fracture: asymptotic analysis. *Int. J. Fract.,* 83, 19–40.

[32] Bazant ZP (2000). Size effect. *Int. J. Solids Struct.,* 37, 69–80.

[33] Taylor D (2007). *The Theory of Critical Distances: A New Perspective in Fracture Mechanics*. Elsevier, London, UK.

[34] Anderson TL (2005). *Fracture mechanics: fundamentals and applications*. CRC Press, Florida, USA.

TABLES

Table 1. Mechanical properties of different non-metallic materials tested. E: Elastic Modulus; $\sigma_{0.2}$: Proof strength; σ_u: ultimate tensile strength; e_{max}: strain under maximum load.

Material	$\sigma_{0.2}$ (MPa)	σ_u (MPa)	E (GPa)	$e_{máx}$ (%)
PMMA	48.5	72.0	3.4	4.05
Granite	9.0	9.0	45.6	-
Limestone	7.8	7.8	64.1	-
PA6	54.2	54.2	2.9	2.07
SGFR-PA6 (5 wt. %) (0 moist %)	66.9	72.1	3.3	2.67
SGFR-PA6 (10 wt. %) (0 moist %)	70.2	78.2	3.6	2.84
SGFR-PA6 (30 wt. %) (0 moist %)	105.4	128.0	6.5	3.56
SGFR-PA6 (50 wt. %) (0 moist %)	161.2	192.8	12.6	2.47
SGFR-PA6 (10 wt. %) (2 moist %)	29.4	63.15	2	18.6
SGFR-PA6 (10 wt. %) (5 moist %)	23.5	47.5	0.95	22.7
SGFR-PA6 (50 wt. %) (2 moist %)	63.25	112.35	7.06	4.09
SGFR-PA6 (50 wt. %) (4 moist %)	46.5	92.27	6.28	5.98

Table 2. Fracture loads.

Material	Specimen	Fracture load (N)	Material	Specimen	Fracture load (N)
PMMA	1	130.03	SGFR-PA6 (30 wt. %) (0 moist %)	1	253.50
	2	83.00		2	195.50
	3	131.23		3	195.70
Granite	1	657.871		4	171.70
	2	538.927		5	180.10
	3	809.095	SGFR-PA6 (50 wt. %) (0 moist %)	1	348.70
	4	660.833		2	351.80
	5	794.461		3	331.80
	6	719.049		4	346.40
Oolitic limestone	1	351.372		5	369.40
	2	392.182	SGFR-PA6 (10 wt. %) (2 moist %)	1	157.90
	3	361.366		2	160.70
	4	386.044		3	173.80
	5	304.196		4	161.10
	6	356.81		5	188.10
PA6	1	92.00	SGFR-PA6 (10 wt. %) (5 moist %)	1	147.10
	2	66.20		2	161.70
	3	110.50		3	153.80
	4	93.20		4	164.00
	5	83.10	SGFR-PA6 (50 wt. %) (2 moist %)	1	345.90
SGFR-PA6 (5 wt. %) (0 moist %)	1	100.50		2	352.80
	2	69.60		3	342.40
	3	73.30		4	296.00
	4	72.00		5	333.00
	5	69.00	SGFR-PA6 (50 wt. %) (4 moist %)	1	234.10
SGFR-PA6 (10 wt. %)	1	117.50		2	211.30
	2	107.20		3	203.30

(0 moist %)	3	70.20	4	231.90
	4	76.70	5	224.50
	5	95.90		

Table 3. Values of N obtained by using the Hollomon equation.

MATERIAL	N, Hollomon
PMMA	0.296
Granite	-
Limestone	-
PA6	-
SGFR-PA6 (5 wt. %) (0 moist %)	0.104
SGFR-PA6 (10 wt. %) (0 moist %)	0.106
SGFR-PA6 (30 wt. %) (0 moist %)	0.116
SGFR-PA6 (50 wt. %) (0 moist %)	0.12
SGFR-PA6 (10 wt. %) (2 moist %)	0.1495
SGFR-PA6 (10 wt. %) (5 moist %)	0.1836
SGFR-PA6 (50 wt. %) (2 moist %)	0.24
SGFR-PA6 (50 wt. %) (4 moist %)	0.25

FIGURE 1

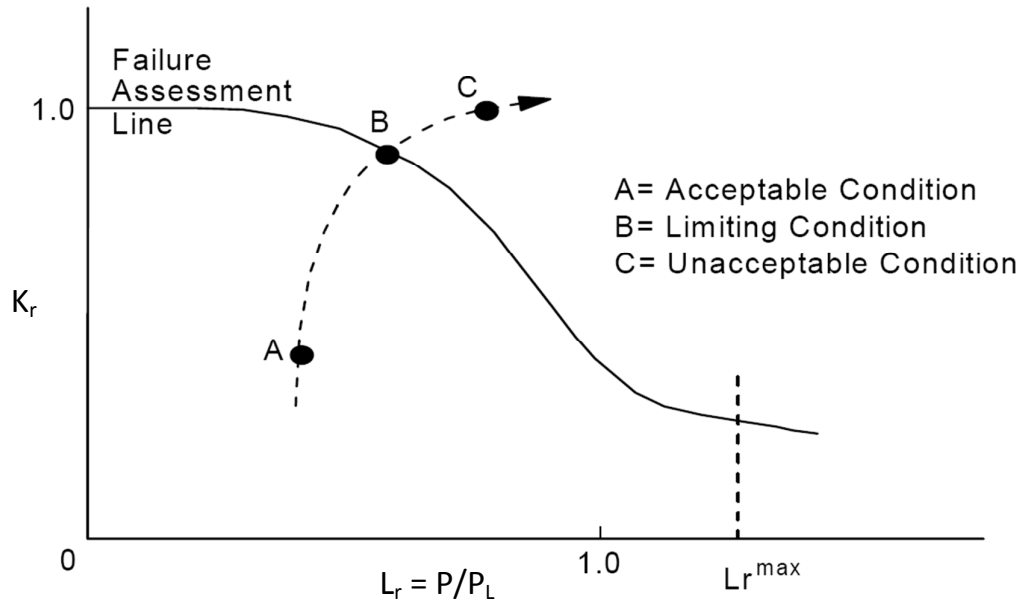

FIGURE 2

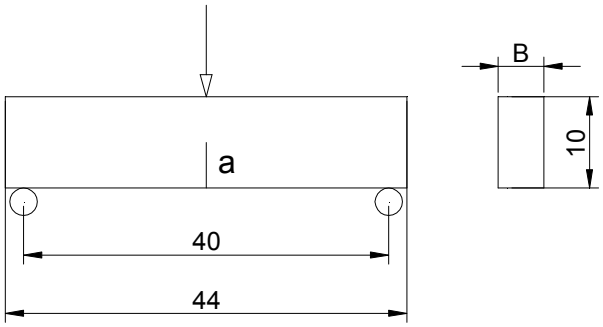

FIGURE 3

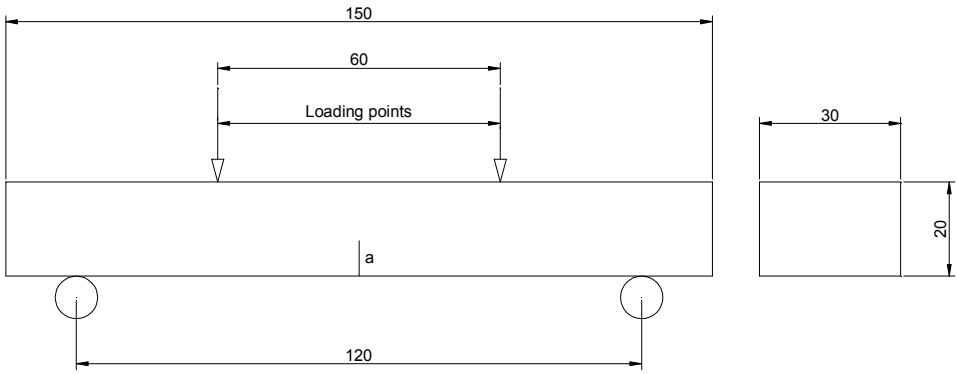

FIGURE 4

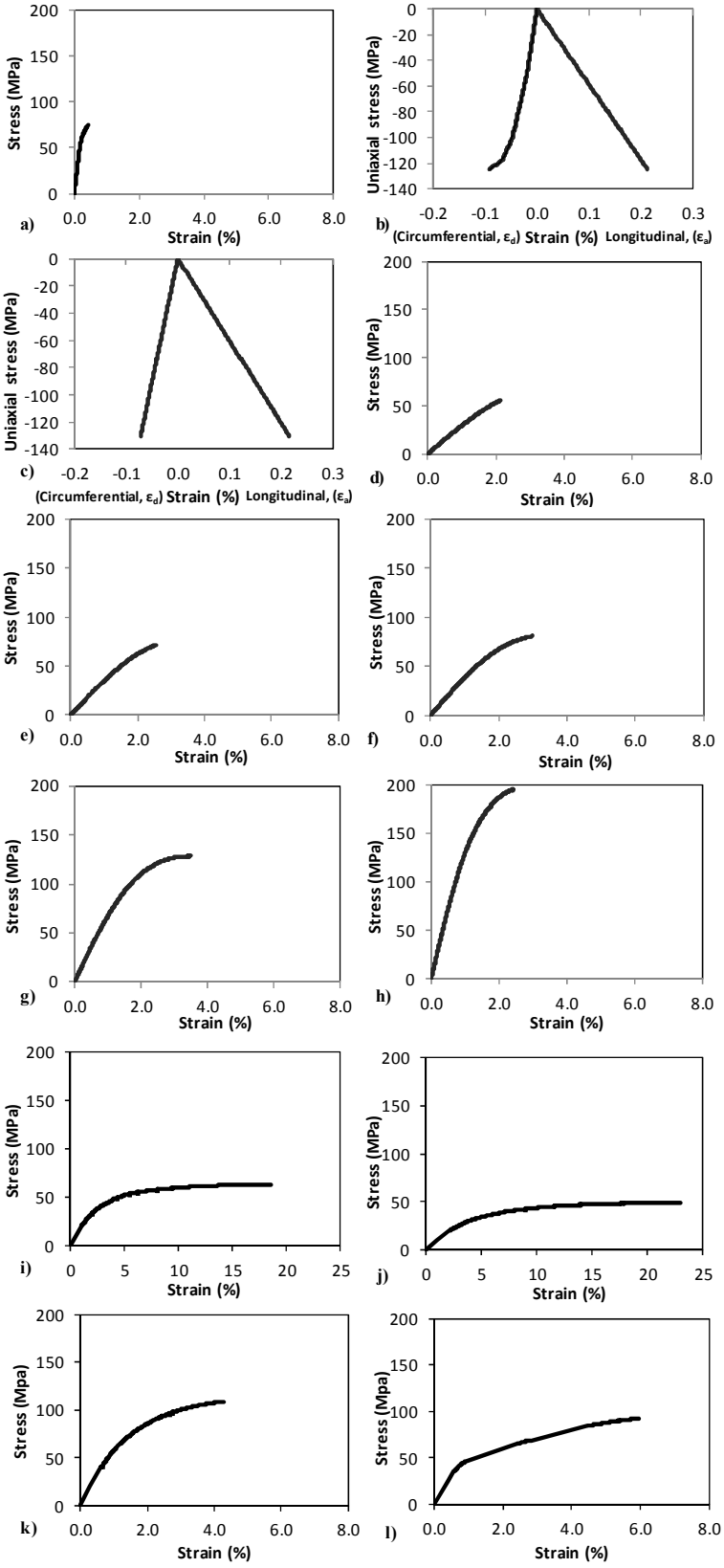
a)
Stress (MPa)
Strain (%)
b)
Uniaxial stress (MPa)
(Circumferential, ε_d) Strain (%) Longitudinal, (ε_a)
c)
Uniaxial stress (MPa)
(Circumferential, ε_d) Strain (%) Longitudinal, (ε_a)
d)
Stress (MPa)
Strain (%)
e)
Stress (MPa)
Strain (%)
f)
Stress (MPa)
Strain (%)
g)
Stress (MPa)
Strain (%)
h)
Stress (MPa)
Strain (%)
i)
Stress (MPa)
Strain (%)
j)
Stress (MPa)
Strain (%)
k)
Stress (Mpa)
Strain (%)
l)
Stress (Mpa)
Strain (%)

FIGURE 5

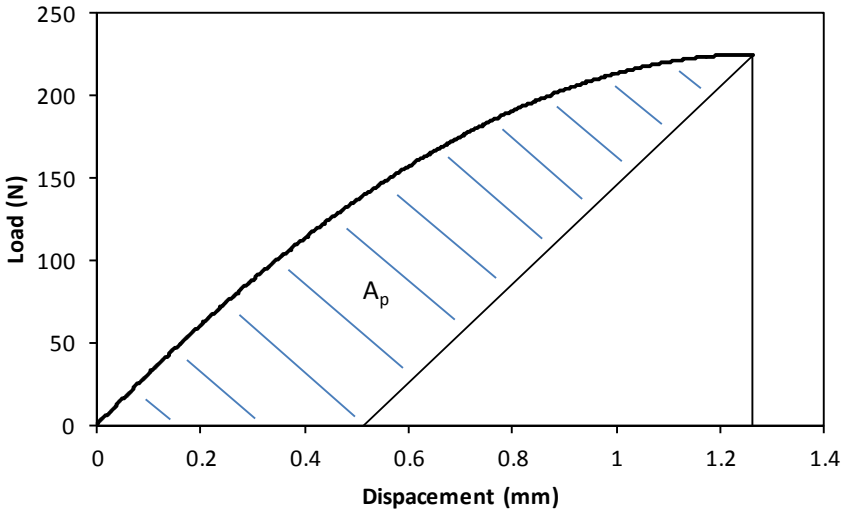

FIGURE 6

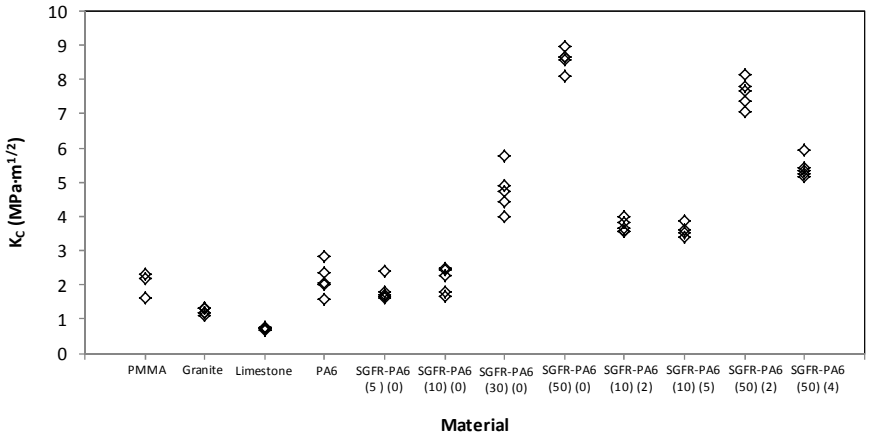

FIGURE 7

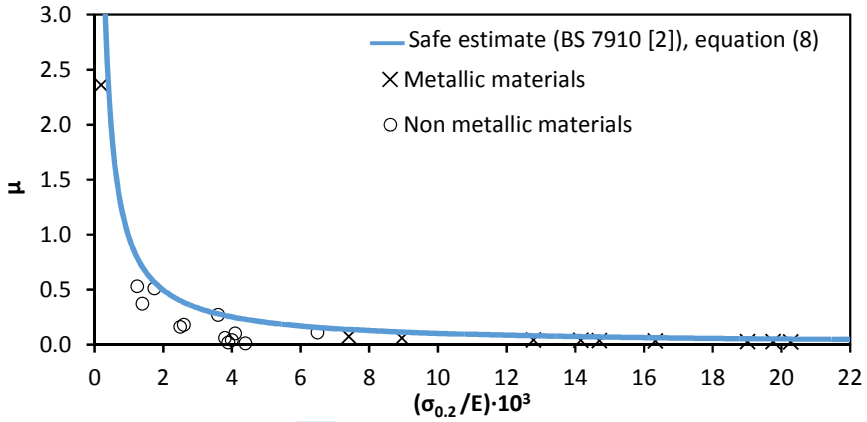

FIGURE 8

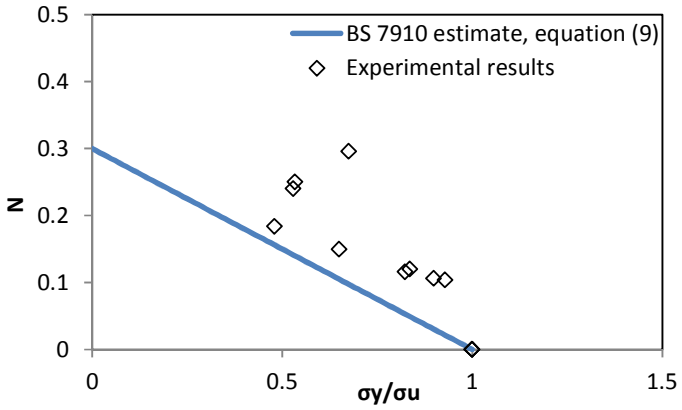

FIGURE 9